Springer

Journal of Mechanical Science and Technology 23 (2009) 1306~1322

Journal of Mechanical Science and Technology

www.springerlink.com/content/1738-494x
DOI 10.1007/s12206-008-1004-6

Characteristics of a transiently propagating crack in functionally graded materials †

Kwang Ho Lee[1,*], Young Jae Lee[2] and Sang Bong Cho[3]

[1]*School of Mechanical and Automotive Engineering, Kyungpook National University, Sangju, Kyeongbuk, 742-711, South Korea*
[2]*Department of Civil Engineering, Kyungpook National University, Sangju, Kyeongbuk, South Korea, 742-711*
[3]*School of Mechanical and Automation, Kyungnam University, Masan, Kyeongnam, South Korea , 631-701*

(Manuscript Received July 14, 2008; Revised August 20, 2008; Accepted October 10, 2008)

Abstract

When a crack propagates with acceleration, deceleration and time rates of change of stress intensity factors, it is very important for us to understand the effects of acceleration, deceleration and time rates of change of stress intensity factors on the individual stresses and displacements at the crack tip. Therefore, the crack tip stress and displacement fields for a transiently propagating crack along gradient in functionally graded materials (FGMs) with an exponential variation of shear modulus and density are developed and the characteristics of a transiently propagating crack from the fields are analyzed. The effects of the rate of change of the stress intensity factor and the crack tip acceleration on the individual stresses at the crack tip are opposite each other. Specially, the isochromatics (constant maximum shear stress) of Mode I tilt backward around the crack tip with an increase of crack tip acceleration, and tilt forward around the crack tip with an increase of the rate of change of the dynamic mode I stress intensity factor.

Keywords: Transiently propagating crack; Accelerating and decelerating crack; Dynamic stress intensity factor; Stress and displacement fields

1. Introduction

The behavior of propagating cracks in functionally graded materials (FGMs) was studied early on by Atkinson and List [1] and many researchers have investigated the behavior of propagating cracks in FGMs.

For the dynamic stress intensity factors of propagating cracks in FGMs, Wang and Meguid [2] studied the propagating cracks by solving the appropriate singular integral equations using Chebyshev polynomials for different inhomogeneous materials under antiplane loading condition. Jiang and Wang [3] studied a finite crack with constant length (Yoffe type crack) propagating in an interfacial layer with spatially varying elastic properties under inplane loading. Ma et al. [4] analyzed for a finite crack with constant length propagating in a functionally graded strip under plane loading by means of the Schmidt method. Cheng and Zhong [5] studied the finite crack with constant length propagating in a functionally graded strip with spatially varying elastic properties between two dissimilar homogeneous layers under inplane loading by utilizing the Fourier transform technique.

For the experimental studies of a propagating crack in FGM, Rousseau and Tippur [6] evaluated the crack tip deformation and fracture parameter histories in compositionally graded glass-filled epoxy under low velocity impact loading. Kirugulige et al. [7] studied experimentally and numerically the model sandwich structures comprising of graded core with bilinear variation of volume fraction of hollow microballoons. Yao et al. [8] studied dynamic crack initiation and

† This paper was recommended for publication in revised form by Associate Editor Chongdu Cho

* Corresponding author. Tel.: +82 54 530 1404, Fax.: +82 54 530 1407
E-mail address: khl@knu.ac.kr

propagation of functionally graded materials (FGMs) using the optical method of caustics.

For the fields of a propagating crack in FGMs, Parameswaran and Shukla [9] developed the higher order fields of the first stress invariant through an asymptotic analysis, and the fields bring out the effects of nonhomogeneity. However, some higher order terms in the fields approach infinity as a crack speed approaches zero as pointed out by Rousseau & Tippur [6] and Kirugulige et al. [7]. This behavior is irregular in physical meaning. Lee [10] developed nonhomogeneous specific terms for individual stress and displacement components that solved the problem. During crack initiating or stopping, the crack propagates at acceleration or deceleration with changing stress intensity factor. To analyze these transient crack states, Freund [11] first developed a higher order expansion of the first stress invariant for isotropic materials during transient crack growth and only square root singular term in the fields cannot completely describe the transiently propagating crack tip state. Rosakis et al. [12] obtained the higher order asymptotic individual stress components near the tip of a non-uniformly propagating mode I crack. Shukla and Jain [13] developed the Mode I stress and displacement fields for a transient crack propagating along the direction of property gradation in FGMs. The contours of constant maximum shear stress (isochromatics) under Mode I tilt forward around the crack tip with the increase of crack tip acceleration $\dot{c}$ ($\mathrm{d}c/\mathrm{d}t$), and tilt backward around the crack tip with the increase of the rate of change of the dynamic mode I stress intensity factor $\dot{K}_I$ ($\mathrm{d}K_I/\mathrm{d}t$). The results are the opposite of those in this study. Chalivendra and Shukla [14] also developed asymptotic expansion of out of plane displacement $w\{\nu, h, (\sigma_{xx}+\sigma_{yy})\}$ when a transient crack propagates arbitrarily in FGMs. The contours of the out of plane displacement become compressed ahead of the crack tip when $\dot{K}_I$ or $\dot{c}$ increases under mode I state. However, the characteristics of the first stress variant $(\sigma_{xx}+\sigma_{yy})$ are different between Shukla & Jain [13] and Chalivendra & Shukla [14] as $\dot{K}_I$ increases. In addition, some terms in the fields [13, 14] approach infinity as a crack speed approaches zero, as pointed out by Chalivendra and Shukla [14], and this irregularity occurs for $c < 0.3c_s$. Therefore, they suggested that the fields should be applied by a remedial approximation for $c < 0.3c_s$. It means that their fields have two different types between $c < 0.3c_s$ and $c > 0.3c_s$. The types of the fields are not complete. Thus, the crack tip fields solved above problems are developed in this study. The higher order terms of the transient stress and displacement fields at crack tip were obtained by transforming the general partial differential equations of the dynamic equilibrium into Laplace's equations whose solutions have harmonic functions. Thus, the fields can be expressed very simply. When a crack propagates with acceleration, deceleration and time rates of change of stress intensity factors, it is very important for us to understand the effects of acceleration, deceleration and time rates of change of stress intensity factors on the individual stresses at crack tip. Using the stress fields developed in this study, effects of acceleration, deceleration and time rates of change of stress intensity factors on the individual $(\sigma_{xx}, \sigma_{yy}, \tau_{xy})$ stresses at crack tip are studied and compared with Shukla & Jain's results [13]. Also, the effects of transients and nonhomogeneity on isochromatics for a propagating crack in FGMs are discussed.

2. Stress and displacement fields for a transient crack propagating under inplane loading

2.1 Formation of equilibrium equations

Lame's constants (λ, μ) and density (ρ) of the FGM are assumed to vary in an exponential manner as given by Eq. (1), whereas Poisson's ratio (ν) is assumed constant.

$$\mu = \mu_0 \exp(\varsigma \mathrm{X}), \quad \lambda = \lambda_0 \exp(\varsigma \mathrm{X}),$$
$$\rho = \rho_0 \exp(\varsigma \mathrm{X}) \tag{1}$$

where X is the reference coordinate, λ_0 and μ_0 denote Lame's constants at $X = 0$, respectively. ς is a nonhomogeneity constant which has the dimension (length)$^{-1}$. The relationship between stresses and strains can be written as

$$\sigma_{XX} = \exp(\varsigma X)\left[(\lambda_0 + 2\mu_0)\varepsilon_{XX} + \lambda_0 \varepsilon_{YY}\right],$$
$$\sigma_{YY} = \exp(\varsigma X)\left[\lambda_0 \varepsilon_{XX} + (\lambda_0 + 2\mu_0)\varepsilon_{YY}\right],$$
$$\tau_{XY} = \exp(\varsigma X)\mu_0 \gamma_{XY} \tag{2}$$

where σ_{ij} and ε_{ij} are the stress and strain components.

It should be noted in this case that the longitudinal and shear wave speeds of the medium are constant. If the deformation is plane strain, the displacements u and v which are derived from dilatational and shear wave potentials Φ and Ψ can be expressed by Eq. (3)

$$u = \frac{\partial \Phi}{\partial X} + \frac{\partial \Psi}{\partial Y} \quad , \quad v = \frac{\partial \Phi}{\partial Y} - \frac{\partial \Psi}{\partial X} \tag{3}$$

The equilibrium in dynamic state is given by Eq. (4)

$$\frac{\partial \sigma_{XX}}{\partial X} + \frac{\partial \tau_{XY}}{\partial Y} = \rho \frac{\partial^2 u}{\partial t^2} \ , \ \frac{\partial \tau_{XY}}{\partial X} + \frac{\partial \sigma_{YY}}{\partial Y} = \rho \frac{\partial^2 v}{\partial t^2} \tag{4}$$

Substituting Eq. (3) into Eq. (2), and substituting Eq. (2) into Eq. (4), the equations for the dynamic state can be obtained as

$$\frac{\partial}{\partial \mathrm{X}} \left\{ (k+2) \nabla^2 \Phi - \frac{\rho_0}{\mu_0} \frac{\partial^2 \Phi}{\partial t^2} \right\} + \frac{\partial}{\partial \mathrm{Y}} \left\{ \nabla^2 \Psi - \frac{\rho_0}{\mu_0} \frac{\partial^2 \Psi}{\partial t^2} \right\} + \varsigma \left\{ k \nabla^2 \Phi + 2 \frac{\partial^2 \Phi}{\partial \mathrm{X}^2} + 2 \frac{\partial^2 \Psi}{\partial \mathrm{X} \partial \mathrm{Y}} \right\} = 0 \tag{5a}$$

$$\frac{\partial}{\partial \mathrm{Y}} \left\{ (k+2) \nabla^2 \Phi - \frac{\rho_0}{\mu_0} \frac{\partial^2 \Phi}{\partial t^2} \right\} - \frac{\partial}{\partial \mathrm{X}} \left\{ \nabla^2 \Psi - \frac{\rho_0}{\mu_0} \frac{\partial^2 \Psi}{\partial t^2} \right\} + \zeta \left\{ 2 \frac{\partial^2 \Phi}{\partial \mathrm{X} \partial \mathrm{Y}} + \frac{\partial^2 \Psi}{\partial \mathrm{Y}^2} - \frac{\partial^2 \Psi}{\partial \mathrm{X}^2} \right\} = 0 \tag{5b}$$

where $k = \lambda_0 / \mu_0$. The moving crack tip coordinates are $x = X - a(t)$, $y = Y$. Where $a(t)$ is the half crack length in center crack or the crack length of an edge crack. When Φ and Ψ have function of position (x, y) and time t at crack tip, Eq. (5) can be transformed as

$$\alpha_l^2 \frac{\partial^2 \Phi}{\partial x^2} + \frac{\partial^2 \Phi}{\partial y^2} + \varsigma \frac{\partial \Phi}{\partial x} + \frac{\varsigma}{k+2} \frac{\partial \Psi}{\partial y} + \frac{\rho_o}{\mu_o (k+2)} \left(\dot{c} \frac{\partial \Phi}{\partial x} + 2c \frac{\partial^2 \Phi}{\partial x \partial t} - \frac{\partial^2 \Phi}{\partial t^2} \right) = 0 \tag{6a}$$

$$\alpha_s^2 \frac{\partial^2 \Psi}{\partial x^2} + \frac{\partial^2 \Psi}{\partial y^2} + \varsigma \frac{\partial \Psi}{\partial x} + \varsigma k \frac{\partial \Phi}{\partial y} + \frac{\rho_o}{\mu_o} \left(\dot{c} \frac{\partial \Psi}{\partial x} + 2c \frac{\partial^2 \Psi}{\partial x \partial t} - \frac{\partial^2 \Psi}{\partial t^2} \right) = 0 \tag{6b}$$

where

$\alpha_l = \sqrt{1 - (c/c_l)^2}$, $\alpha_s = \sqrt{1 - (c/c_s)^2}$,

$c_s = \sqrt{\mu_c / \rho_c}$,

$c_l = c_s \sqrt{2(1-\nu)/(1-2\nu)}$ for plane strain ,

$c_l = c_s \sqrt{2/(1-\nu)}$ for plane stress.

c , c_l and c_s are the crack propagation velocity, elastic dilatational wave velocity and elastic shear wave velocity at the crack tip. It is very difficult to obtain analytical solutions for the elastodynamic differential Eq. (6). Thus, an asymptotic expansion analysis is used to expand the stress fields around a transiently propagating crack tip. To obtain an asymptotic expansion of the fields around the crack tip, we assume the general solutions of Eq. (6) for $\Phi(z_l, t)$ and $\Psi(z_s, t)$ as follows:

$$\Phi_n(z_l, t) = -\int \phi_n(z_l, t) dz_l \ ,$$

$$\Psi_n(z_s, t) = -\int \psi_n(z_s, t) dz_s \tag{7}$$

And $\phi_n(z_l, t)$ and $\psi_n(z_s, t)$ can be expended by power series as

$$\phi_n(z_l, t) = \sum_{n=1}^{\infty} A_n(t) z_l^{n/2} \ ,$$

$$\psi_n(z_s, t) = \sum_{n=1}^{\infty} B_n(t) z_s^{n/2} \tag{8}$$

where $A_n(t) = A_n^o(t) + i A_n^*(t)$,

$B_n(t) = B_n^o(t) + i B_n^*(t)$, $z_{l(s)} = x + m_{l(s)} y$.

When $\Phi(z_l, t)$ and $\Psi(z_s, t)$ in Eq. (6) can be expanded by powers as Eq. (8), the structure of Eq. (6) can be expressed as Eq. (9)

$$\alpha_l^2 \frac{\partial^2 \Phi_n}{\partial x^2} + \frac{\partial^2 \Phi_n}{\partial y^2} = 0 : \ n = 1, \ 2 \tag{9a}$$

$$\alpha_s^2 \frac{\partial^2 \Psi_n}{\partial x^2} + \frac{\partial^2 \Psi_n}{\partial y^2} = 0 : \ n = 1, \ 2 \tag{9b}$$

$$\alpha_l^2 \frac{\partial^2 \Phi_n}{\partial x^2} + \frac{\partial^2 \Phi_n}{\partial y^2} = -\varsigma \left[\frac{\partial \Phi_{n-2}}{\partial x} + \frac{1}{k+2} \frac{\partial \Psi_{n-2}}{\partial y} \right] - \frac{2c^{1/2}}{c_l^2} \frac{\partial}{\partial t} \left(c^{1/2} \frac{\partial \Phi_{n-2}}{\partial x} \right) : \ n = 3, \ 4 \tag{10a}$$

$$\alpha_s^2\frac{\partial^2\Psi_n}{\partial x^2}+\frac{\partial^2\Psi_n}{\partial y^2}=-\zeta\left[\frac{\partial\Psi_{n-2}}{\partial x}+k\frac{\partial\Phi_{n-2}}{\partial y}\right]$$
$$-\frac{2c^{1/2}}{c_s^2}\frac{\partial}{\partial t}\left(c^{1/2}\frac{\partial\Psi_{n-2}}{\partial x}\right)\ :\ n=3,\ 4 \tag{10b}$$

and so on.

Thus, for any value of n, the equilibrium equation has the general form as

$$\alpha_l^2\frac{\partial^2\Phi_n}{\partial x^2}+\frac{\partial^2\Phi_n}{\partial y^2}=-\zeta\left[\frac{\partial\Phi_{n-2}}{\partial x}+\frac{1}{k+2}\frac{\partial\Psi_{n-2}}{\partial y}\right]$$
$$-\frac{2c^{1/2}}{c_l^2}\frac{\partial}{\partial t}\left(c^{1/2}\frac{\partial\Phi_{n-2}}{\partial x}\right)+\frac{1}{c_l^2}\frac{\partial^2\Phi_{n-4}}{\partial t^2} \tag{11a}$$

$$\alpha_s^2\frac{\partial^2\Psi_n}{\partial x^2}+\frac{\partial^2\Psi_n}{\partial y^2}=-\zeta\left[\frac{\partial\Psi_{n-2}}{\partial x}+k\frac{\partial\Phi_{n-2}}{\partial y}\right]$$
$$-\frac{2c^{1/2}}{c_s^2}\frac{\partial}{\partial t}\left(c^{1/2}\frac{\partial\Psi_{n-2}}{\partial x}\right)+\frac{1}{c_s^2}\frac{\partial^2\Psi_{n-4}}{\partial t^2} \tag{11b}$$

when $n<0$, $\Phi_n=\Psi_n=0$.

2.2 The stress and displacement fields for n =1, 2

Eq. (9) is the Laplace's equation in complex domain $z_{l(s)}=x+m_{l(s)}y$ and the same as that for a homogeneous material and can be rewritten as

$$(\alpha_l^2+m_l^2)\Phi_n^{*}(z_l,t)=0\ \&\ (\alpha_s^2+m_s^2)\Psi_n^{*}(z_s,t)=0\ .$$

Thus $m_{l(s)}=i\alpha_{l(s)}$. The solutions for in Eq. (9) can be expressed as $\Phi_n(z_l,t)=-\mathrm{Re}\int\phi_n(z_l,t)dz_l$ and $\Psi_n(z_s,t)=-\mathrm{Im}\int\psi_n(z_s,t)dz_s$ respectively.

Substituting the differentiation of Φ_n and Ψ_n into Eq. (3), the displacements u and v for $n=1$ and 2 can be expressed as Eq. (12).

$$u=-\mathrm{Re}\{\phi_n(z_l,t)+\alpha_s\psi_n(z_s,t)\}\ ,$$
$$v=\mathrm{Im}\{\alpha_l\phi_n(z_l,t)+\psi_n(z_s,t)\} \tag{12}$$

Substituting the differentiation of Eq. (12) into Eq. (2), the stress σ_{ij} for $n=1$ and 2 can be expressed as Eq. (13).

$$\sigma_{xx}=-\mu\,\mathrm{Re}\{(1+2\alpha_l^2-\alpha_s^2)\phi_n^{'}(z_l,t)+2\alpha_s\psi_n^{'}(z_s,t)\}$$
$$\sigma_{yy}=\mu\,\mathrm{Re}\{(1+\alpha_s^2)\phi_n^{'}(z_l,t)+2\alpha_s\psi_n^{'}(z_s,t)\}$$
$$\tau_{xy}=\mu\,\mathrm{Im}\{2\alpha_l\phi_n^{'}(z_l,t)+(1+\alpha_s^2)\psi_n^{'}(z_s,t)\} \tag{13}$$

Substituting Eq. (8) into Eq. (13), and substituting Eq. (13) into Eq. (2), applying traction free boundary conditions on the crack surface, A_n and B_n can be obtained as

$$A_n^o(t)=-\frac{2}{\mu_c\sqrt{2\pi}}B_I(c)K_n^o(t)\ ,$$
$$A_n^*(t)=\frac{2}{\mu_c\sqrt{2\pi}}B_{II}(c)K_n^*(t),$$
$$B_n^o(t)=\frac{2}{\mu_c\sqrt{2\pi}}h_n^oB_I(c)K_n^o(t),$$
$$B_n^*(t)=-\frac{2}{\mu_c\sqrt{2\pi}}h_n^*B_{II}(c)K_n^*(t) \tag{14}$$

where μ_c is the shear modulus at crack tip.

$$B_I(c)=\frac{1+\alpha_s^2}{4\alpha_l\alpha_s-(1+\alpha_s^2)^2},$$
$$B_{II}(c)=\frac{2\alpha_s}{4\alpha_l\alpha_s-(1+\alpha_s^2)^2},$$
$$h_1^o=h_2^*=\frac{2\alpha_l}{1+\alpha_s^2}\ ,\ \ h_1^*=h_2^o=\frac{1+\alpha_s^2}{2\alpha_s}\ .$$

Substituting Eq. (14) into Eq.(7), and substituting Eq. (7) into Eq. (2) and (3), the stresses and displacements for a propagating crack are obtained in Eqs. (15) and (16).

$$\sigma_{xxn}=\exp(\varsigma x)\sum_{n=1}^{2}\sigma_{xxn}^o\ ,\ \ \sigma_{yyn}=\exp(\varsigma x)\sum_{n=1}^{2}\sigma_{yyn}^o\ ,$$
$$\tau_{xyn}=\exp(\varsigma x)\sum_{n=1}^{2}\tau_{xyn}^o \tag{15}$$

where

$$\sigma_{xxn}^o=\frac{K_n^o(t)B_I(c)}{\sqrt{2\pi}}n\left\{(1+2\alpha_l^2-\alpha_s^2)r_l^{\frac{n-2}{2}}\cos(\frac{n-2}{2})\theta_l-\right.$$
$$\left.2\alpha_sh_n^or_s^{\frac{n-2}{2}}\cos(\frac{n-2}{2})\theta_s\right\}$$

$$\sigma_{xxn}=\frac{K_n^oB_I(c)}{\sqrt{2\pi}}n\left\{(1+2\alpha_l^2-\alpha_s^2)r_l^{\frac{n-2}{2}}\cos(\frac{n-2}{2})\theta_l-\right.$$
$$\left.2\alpha_sh_n^or_s^{\frac{n-2}{2}}\cos(\frac{n-2}{2})\theta_s\right\}$$

$$+\frac{K_n^*(t)B_{II}(c)}{\sqrt{2\pi}}n\left\{(1+2\alpha_l^2-\alpha_s^2)r_l^{\frac{n-2}{2}}\sin(\frac{n-2}{2})\theta_l - 2\alpha_s h_n^* r_s^{\frac{n-2}{2}}\sin(\frac{n-2}{2})\theta_s\right\}$$

$$+\frac{K_n^* B_{II}(c)}{\sqrt{2\pi}}n\left\{(1+2\alpha_l^2-\alpha_s^2)r_l^{\frac{n-2}{2}}\sin(\frac{n-2}{2})\theta_l - 2\alpha_s h_n^* r_s^{\frac{n-2}{2}}\sin(\frac{n-2}{2})\theta_s\right\}$$

$$\sigma_{yyn}^o=\frac{K_n^o(t)B_I(c)}{\sqrt{2\pi}}n\left\{-(1+\alpha_s^2)r_l^{\frac{n-2}{2}}\cos(\frac{n-2}{2})\theta_l + 2\alpha_s h_n^o r_s^{\frac{n-2}{2}}\cos(\frac{n-2}{2})\theta_s\right\}$$

$$\sigma_{yyn}=\frac{K_n^o B_I(c)}{\sqrt{2\pi}}n\left\{-(1+\alpha_s^2)r_l^{\frac{n-2}{2}}\cos(\frac{n-2}{2})\theta_l + 2\alpha_s h_n^o r_s^{\frac{n-2}{2}}\cos(\frac{n-2}{2})\theta_s\right\}$$

$$+\frac{K_n^*(t)B_{II}(c)}{\sqrt{2\pi}}n\left\{-(1+\alpha_s^2)r_l^{\frac{n-2}{2}}\sin(\frac{n-2}{2})\theta_l + 2\alpha_s h_n^* r_s^{\frac{n-2}{2}}\sin(\frac{n-2}{2})\theta_s\right\}$$

$$+\frac{K_n^* B_{II}(c)}{\sqrt{2\pi}}n\left\{-(1+\alpha_s^2)r_l^{\frac{n-2}{2}}\sin(\frac{n-2}{2})\theta_l + 2\alpha_s h_n^* r_s^{\frac{n-2}{2}}\sin(\frac{n-2}{2})\theta_s\right\}$$

$$\tau_{xyn}^o=\frac{K_n^o(t)B_I(c)}{\sqrt{2\pi}}n\left\{-2\alpha_l r_l^{\frac{n-2}{2}}\sin(\frac{n-2}{2})\theta_l + (1+\alpha_s^2)h_n^o r_s^{\frac{n-2}{2}}\sin(\frac{n-2}{2})\theta_s\right\}$$

$$\tau_{xyn}=\frac{K_n^o B_I(c)}{\sqrt{2\pi}}n\left\{-2\alpha_l r_l^{\frac{n-2}{2}}\sin(\frac{n-2}{2})\theta_l + (1+\alpha_s^2)h_n^o r_s^{\frac{n-2}{2}}\sin(\frac{n-2}{2})\theta_s\right\}$$

$$+\frac{K_n^*(t)B_{II}(c)}{\sqrt{2\pi}}n\left\{2\alpha_l r_l^{\frac{n-2}{2}}\cos(\frac{n-2}{2})\theta_l - (1+\alpha_s^2)h_n^* r_s^{\frac{n-2}{2}}\cos(\frac{n-2}{2})\theta_s\right\}$$

$$+\frac{K_n^* B_{II}(c)}{\sqrt{2\pi}}n\left\{2\alpha_l r_l^{\frac{n-2}{2}}\cos(\frac{n-2}{2})\theta_l - (1+\alpha_s^2)h_n^* r_s^{\frac{n-2}{2}}\cos(\frac{n-2}{2})\theta_s\right\}$$

$$u_n=\exp(-\varsigma a)\sum_{n=1}^{2}u_n^o\ ,\quad v_n=\exp(-\varsigma a)\sum_{n=1}^{2}v_n^o \tag{16}$$

where

$$u_n^o=\frac{K_n^o(t)B_I(c)}{\mu_o}\sqrt{\frac{2}{\pi}}\left\{r_l^{\frac{n}{2}}\cos(\frac{n}{2})\theta_l-\alpha_s h_n^o r_s^{\frac{n}{2}}\cos(\frac{n}{2})\theta_s\right\}$$

$$+\frac{K_n^*(t)B_{II}(c)}{\mu_o}\sqrt{\frac{2}{\pi}}\left\{r_l^{\frac{n}{2}}\sin(\frac{n}{2})\theta_l-\alpha_s h_n^* r_s^{\frac{n}{2}}\sin(\frac{n}{2})\theta_s\right\},$$

$$v_n^o=\frac{K_n^o(t)B_I(c)}{\mu_o}\sqrt{\frac{2}{\pi}}\left\{-\alpha_l r_l^{\frac{n}{2}}\sin(\frac{n}{2})\theta_l+h_n^o r_s^{\frac{n}{2}}\sin(\frac{n}{2})\theta_s\right\}$$

$$+\frac{K_n^*(t)B_{II}(c)}{\mu_o}\sqrt{\frac{2}{\pi}}\left\{\alpha_l r_l^{\frac{n}{2}}\cos(\frac{n}{2})\theta_l-h_n^* r_s^{\frac{n}{2}}\cos(\frac{n}{2})\theta_s\right\}$$

$r_j=\sqrt{x^2+(\alpha_j y)^2}$, $\theta_j=\tan^{-1}(\alpha_j y/x)$, $j=l,s$.

$K_1^o(t)$ and $K_1^*(t)$ for $n=1$ denote the stress intensity factors $K_I(t)$ and $K_{II}(t)$, respectively.

When $n=1$ and 2, the differential equations in Eq. (9) are the same as those for a homogeneous material [11] but their stress and displacement fields are influenced by the nonhomogeneity constant ς. When ς is zero, Eqs. (15) and (16) are the same as those [11, 15] of homogeneous materials.

2.3 Stress and displacement fields for n =3 and 4

For $n\geq 3$ in Eq. (10), the $\Phi_n(z_l,t)$ and $\Psi_n(z_s,t)$ have nonhomogeneous coefficients and transient terms, and only $n=3$ and 4 are considered to generate the fields in this study.

The relation between $\Phi_{n-2}(z_l,t)$ and $\Psi_{n-2}(z_s,t)$ in Eq. (10) can be written as [10].

$$\frac{\partial}{\partial y}\Psi_{n-2}(z_s,t)=-(k+2)\frac{\partial}{\partial x}\Phi_{n-2}(z_l,t)\ ,$$

$$\frac{1}{k+2}\frac{\partial}{\partial x}\Psi_{n-2}(z_s,t)=\frac{\partial}{\partial y}\Phi_{n-2}(z_l,t) \tag{17}$$

Substituting Eq. (17) into Eqs. (10a) and (10b), Eqs. (10a) and (10b) can be written as

$$\alpha_l^2\frac{\partial^2\Phi_n}{\partial x^2}+\frac{\partial^2\Phi_n}{\partial y^2}=-\frac{2c^{1/2}}{c_l^2}\frac{\partial}{\partial t}\left(c^{1/2}\frac{\partial\Phi_{n-2}}{\partial x}\right) \tag{18a}$$

$$\alpha_s^2\frac{\partial^2\Psi_n}{\partial x^2}+\frac{\partial^2\Psi_n}{\partial y^2}=-\varsigma\left[D_s\frac{\partial\Psi_{n-2}}{\partial x}\right] -\frac{2c^{1/2}}{c_s^2}\frac{\partial}{\partial t}\left(c^{1/2}\frac{\partial\Psi_{n-2}}{\partial x}\right) \tag{18b}$$

where $D_s = 1 + k/(k+2) = 2(\alpha_l^2 - \alpha_s^2)/(1-\alpha_s^2)$

Substituting Eqs. (7) and (8) into Eq. (18), Eq. (19) can be obtained as

$$\left\{\frac{n}{2}(\alpha_l^2 + m_l^2)A_n(t)z_l^{n/2-1} = -\frac{2c^{1/2}}{c_l^2}\frac{\partial}{\partial t}\left(c^{1/2}A_{n-2}(t)z_l^{n/2-1}\right)\right\} \quad (19a)$$

$$\left\{\frac{n}{2}(\alpha_s^2 + m_s^2)B_n(t)z_s^{n/2-1} = -\varsigma D_s B_{n-2}z_s^{n/2-1} - \frac{2c^{1/2}}{c_s^2}\frac{\partial}{\partial t}\left(c^{1/2}B_{n-2}(t)z_s^{n/2-1}\right)\right\} \quad (19b)$$

when $n \geq 3$, m_l and m_s are dependent on the crack propagation, physical properties, nonhomo-geneity and acceleration, and the value is changed for each n. From Eq. (19), m_l and m_s can be written as

$$m_l = i\hat{\alpha}_l, \quad m_s = i\hat{\alpha}_s \quad (20)$$

For Mode I ;

$$\hat{\alpha}_l = \sqrt{\alpha_l^2 + k_n^o \frac{2}{n}\frac{c}{c_l^2}\left(\frac{\dot{c}}{c} + 2\frac{\dot{A}_{n-2}^o}{A_{n-2}^o} + \delta_l(n)\right)},$$

$$\hat{\alpha}_s = \sqrt{\alpha_s^2 + k_n^o \frac{2}{n}\left(\varsigma D_s + \frac{c}{c_s^2}[\frac{\dot{c}}{c} + 2\frac{\dot{B}_{n-2}^o}{B_{n-2}^o} + \delta_s(n)]\right)},$$

$$k_n^o = A_{n-2}^o(t)/A_n^o(t) = B_{n-2}^o(t)/B_n^o(t),$$

$$\delta_l(3) = \frac{2\dot{\alpha}_l}{\alpha_l}\sin^2\frac{\theta_l}{2}, \quad \delta_s(3) = \frac{2\dot{\alpha}_s}{\alpha_s}\cos^2\frac{\theta_s}{2},$$

$$\delta_l(4) = 0, \quad \delta_s(4) = 2\dot{\alpha}_s/\alpha_s,$$

For Mode II ;

$$\hat{\alpha}_l = \sqrt{\alpha_l^2 + k_n^* \frac{2}{n}\frac{c}{c_l^2}\left(\frac{\dot{c}}{c} + 2\frac{\dot{A}_{n-2}^*}{A_{n-2}^*} + \delta_l(n)\right)},$$

$$\hat{\alpha}_s = \sqrt{\alpha_s^2 + k_n^* \frac{2}{n}\left(\varsigma D_s + \frac{c}{c_s^2}[\frac{\dot{c}}{c} + 2\frac{\dot{B}_{n-2}^*}{B_{n-2}^*} + \delta_s(n)]\right)},$$

$$k_n^* = A_{n-2}^*(t)/A_n^*(t) = B_{n-2}^*(t)/B_n^*(t),$$

$$\delta_l(3) = \frac{2\dot{\alpha}_l}{\alpha_l}\cos^2\frac{\theta_l}{2}, \quad \delta_s(3) = \frac{2\dot{\alpha}_s}{\alpha_s}\sin^2\frac{\theta_s}{2},$$

$$\delta_l(4) = 2\dot{\alpha}_l/\alpha_l, \quad \delta_s(4) = 0.$$

$$\dot{A}_{n-2}^o(t) = -\frac{2}{\mu_c\sqrt{2\pi}}\left[\frac{2\alpha_s\dot{\alpha}_s D - (1+\alpha_s^2)\dot{D}}{D^2}K_{n-2}^o(t) + \frac{1+\alpha_s^2}{D}\dot{K}_{n-2}^o(t)\right],$$

$$\dot{B}_{n-2}^o(t) = \frac{2}{\mu_c\sqrt{2\pi}}\left[\frac{2\dot{\alpha}_l D - 2\alpha_l\dot{D}}{D^2}K_{n-2}^o(t) + \frac{2\alpha_l}{D}\dot{K}_{n-2}^o(t)\right],$$

$$D = 4\alpha_l\alpha_s - (1+\alpha_s^2)^2,$$

$$\dot{D} = -4c\dot{c}\left[\frac{\alpha_s}{\alpha_l c_l^2} + \frac{\alpha_l}{\alpha_s c_s^2} - \frac{1+\alpha_s^2}{c_s^2}\right],$$

$$\dot{A}_{n-2}^*(t) = \frac{2}{\mu_c\sqrt{2\pi}}\left[\frac{2\dot{\alpha}_s D - 2\alpha_s\dot{D}}{D^2}K_{n-2}^*(t) + \frac{2\alpha_s}{D}\dot{K}_{n-2}^*(t)\right],$$

$$\dot{B}_{n-2}^*(t) = -\frac{2}{\mu_c\sqrt{2\pi}}\left[\frac{2\alpha_s\dot{\alpha}_s D - (1+\alpha_s^2)\dot{D}}{D^2}K_{n-2}^*(t) + \frac{1+\alpha_s^2}{D}\dot{K}_{n-2}^*(t)\right],$$

$$\dot{c} = \mathrm{d}c/\mathrm{d}t, \quad \dot{\alpha}_s = \frac{-c\dot{c}}{\alpha_s c_s^2}, \quad \dot{\alpha}_l = \frac{-c\dot{c}}{\alpha_l c_l^2},$$

$$\dot{K}_n^{o(*)} = \mathrm{d}K_n^{o(*)}/\mathrm{d}t, \quad K_I^o(t) = K_I(t),$$

$K_I^*(t) = K_{II}(t)$. $m_j(=i\hat{\alpha}_j)$ in Eq. (20) is dependent on crack propagation velocity (c), acceleration ($\dot{c}$), rate of change of the stress intensity factor [$\dot{K}(dK/dt)$], physical properties (c_l, c_s), nonhomogeneity (ς) and angle (θ) at the crack tip. The unit of k_n^o and k_n^* is length. When $n = 4$ or the transient crack propagates at constant velocity, m_l and m_s are independent of x and y. When $n = 3$, if the transient crack propagates at nonuniform speed, the value of $\delta_{l(s)}(3)$ which is related to θ in $\hat{\alpha}_j(j = l,s)$ is nonzero. However, $\delta_{l(s)}(3)$ is very small compared to the other terms.

Fig. 1 shows $m_j(\theta)/m_j(c)$ for $n = 3$, in which $m_j(c)$ is $m_j(c, \delta_{l(s)}(3) = 0)$. As shown in Fig. 1, $m_j(\theta)/m_j(c)$ approaches one. This indicates that $\delta_{l(s)}(3)$ almost does not influence $\hat{\alpha}_j(j = l,s)$. Thus, we assume that the m_j is independent of x and y. When m_l and m_s are the same as Eq. (20), Eq. (18) can expressed as Eq. (21)

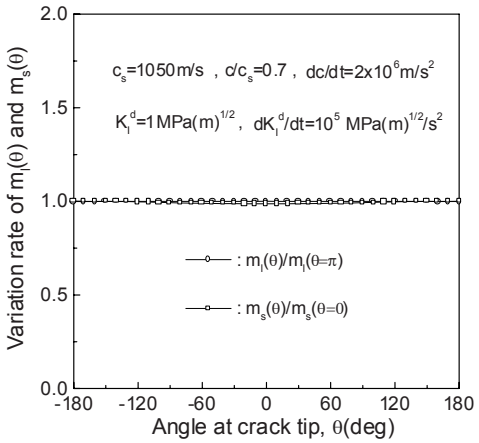

Fig. 1. Variation in the rate of $m_l(\theta)$ and $m_s(\theta)$ with angle at crack tip for $\varsigma = 4$ and $k_3^o > 10^{-4}$m .

$$\hat{\alpha}_l^2 \frac{\partial^2 \Phi_n(\hat{z}_l,t)}{\partial x^2} + \frac{\partial^2 \Phi_n(\hat{z}_l,t)}{\partial y^2} = 0$$
$$\hat{\alpha}_s^2 \frac{\partial^2 \Psi_n(\hat{z}_s,t)}{\partial x^2} + \frac{\partial^2 \Psi_n(\hat{z}_s,t)}{\partial y^2} = 0 \qquad (21)$$

where $\hat{z}_j = x + i\hat{\alpha}_j y$ and $\hat{\alpha}_j$ is dependent on transients in addition to physical properties and crack propagation velocity. Eq. (21) is also Laplace's equation in complex domain $\hat{z}_j$ and can be rewritten as $(\hat{\alpha}_l^2 + m_l^2)\Phi_n^{"}(\hat{z}_l) = 0$ & $(\hat{\alpha}_s^2 + m_s^2)\Psi_n^{"}(\hat{z}_s) = 0$. Thus, $m_l = i\hat{\alpha}_l$ and $m_s = i\hat{\alpha}_s$. When $n > 3$, Laplace's equations for $\Phi_n(\hat{z}_l,t)$ and $\Psi_n(\hat{z}_s,t)$ can be also obtained and the solutions of the Laplace's equations have harmonic functions. Thus, $\Phi_n(\hat{z}_l,t)$ and $\Psi_n(\hat{z}_s,t)$ can be written as

$$\Phi_n(\hat{z}_l,t) = -\mathrm{Re}\int \phi_n(\hat{z}_l,t)d\hat{z}_l \ ,$$
$$\Psi_n(\hat{z}_s,t) = -\mathrm{Im}\int \psi_n(\hat{z}_s,t)d\hat{z}_s \qquad (22)$$

where

$\hat{r}_j = \sqrt{x^2 + (\hat{\alpha}_j y)^2}$, $\hat{\theta}_j = \tan^{-1}[\hat{\alpha}_j y / x]$, $j = l, s$.

$\phi_n(\hat{z}_l)$ and $\psi_n(\hat{z}_s)$ are dependent on acceleration(dc/dt) and the rate of change of the stress intensity factor ($\mathrm{d}K/\mathrm{d}t$) in addition to the crack propagation velocity and physical properties. Substituting the differentiation of $\Phi_n(\hat{z}_l)$ and $\Psi_n(\hat{z}_s)$ in Eq. (22) into Eq. (3), the displacements u and v for $n = 3,\ 4$ can be expressed as Eq. (23).

$$u = -\mathrm{Re}\{\phi_n(\hat{z}_l,t) + \hat{\alpha}_s\psi_n(\hat{z}_s,t)\} \ ,$$
$$v = \mathrm{Im}\{\hat{\alpha}_l\phi_n(\hat{z}_l,t) + \psi_n(\hat{z}_s,t)\} \qquad (23)$$

Substituting the differentiation of Eq. (23) into Eq. (2), the stress σ_{ij} for $n = 3,\ 4$ can be expressed as Eq. (24).

$$\sigma_{xx} = -\mu\mathrm{Re}\left\{\left[\frac{1-\alpha_s^2}{1-\alpha_l^2}(1-\hat{\alpha}_l^2) + 2\hat{\alpha}_l^2\right]\phi_3'(\hat{z}_l,t) + 2\hat{\alpha}_s\psi_3'(\hat{z}_s,t)\right\}$$
$$\sigma_{yy} = \mu\mathrm{Re}\left\{\left[-\frac{1-\alpha_s^2}{1-\alpha_l^2}(1-\hat{\alpha}_l^2) + 2\right]\phi_3'(\hat{z}_l,t) + 2\hat{\alpha}_s\psi_3'(\hat{z}_s,t)\right\}$$
$$\tau_{xy} = \mu\,\mathrm{Im}\left\{2\hat{\alpha}_l\phi_n'(\hat{z}_l,t) + (1+\hat{\alpha}_s^2)\psi_n'(\hat{z}_s,t)\right\} \qquad (24)$$

The $\phi_n(\hat{z}_l,t)$ and $\psi_n(\hat{z}_s,t)$ can be written as

$$\phi_n(\hat{z}_l,t) = \sum_{n=3}^{4}[\hat{A}_n^o(t) + \hat{A}_n^*(t)]\hat{z}_l^{n/2}$$
$$\psi_n(\hat{z}_s,t) = \sum_{n=3}^{4}[\hat{B}_n^o(t) + \hat{B}_n^*(t)]\hat{z}_s^{n/2} \qquad (25)$$

Substituting Eq. (25) into Eq. (24), the stress fields become

$$\begin{aligned}
\sigma_{xxn} = &-\sum_{n=3}^{4}\mu\frac{n}{2}\left\{\hat{A}_n^o(t)\left[\frac{1-\alpha_s^2}{1-\alpha_l^2}(1-\hat{\alpha}_l^2) + 2\hat{\alpha}_l^2\right]\hat{r}_l^{(n-2)/2}\right.\\
&\left.\times\cos(\frac{n-2}{2})\hat{\theta}_l + 2\hat{B}_n^o(t)\hat{\alpha}_s\hat{r}_s^{(n-2)/2}\cos(\frac{n-2}{2})\hat{\theta}_s\right\}\\
&+\sum_{n=3}^{4}\mu\frac{n}{2}\left\{\hat{A}_n^*(t)\left[\frac{1-\alpha_s^2}{1-\alpha_l^2}(1-\hat{\alpha}_l^2) + 2\hat{\alpha}_l^2\right]\hat{r}_l^{(n-2)/2}\right.\\
&\left.\times\sin(\frac{n-2}{2})\hat{\theta}_l + 2\hat{B}_n^*(t)\hat{\alpha}_s\hat{r}_s^{(n-2)/2}\sin(\frac{n-2}{2})\hat{\theta}_s\right\}\\
\sigma_{yyn} = &\sum_{n=3}^{4}\mu\frac{n}{2}\left\{\hat{A}_n^o(t)\left[-\frac{1-\alpha_s^2}{1-\alpha_l^2}(1-\hat{\alpha}_l^2) + 2\right]\hat{r}_l^{(n-2)/2}\right.\\
&\left.\times\cos(\frac{n-2}{2})\hat{\theta}_l + 2\hat{B}_n^o(t)\hat{\alpha}_s\hat{r}_s^{(n-2)/2}\cos(\frac{n-2}{2})\hat{\theta}_s\right\}\\
&-\sum_{n=3}^{4}\mu\frac{n}{2}\left\{\hat{A}_n^*(t)\left[-\frac{1-\alpha_s^2}{1-\alpha_l^2}(1-\hat{\alpha}_l^2) + 2\right]\hat{r}_l^{(n-2)/2}\right.\\
&\left.\times\sin(\frac{n-2}{2})\hat{\theta}_l + 2\hat{B}_n^*(t)\hat{\alpha}_s\hat{r}_s^{(n-2)/2}\sin(\frac{n-2}{2})\hat{\theta}_s\right\}\\
\tau_{xyn} = &\sum_{n=3}^{4}\mu\frac{n}{2}\left\{\hat{A}_n^o(2\hat{\alpha}_l)\hat{r}_l^{(n-2)/2}\sin(\frac{n-2}{2})\hat{\theta}_l\right.\\
&\left.+\hat{B}_n^o(t)(1+\hat{\alpha}_s^2)\hat{r}_s^{(n-2)/2}\sin(\frac{n-2}{2})\hat{\theta}_s\right\}\\
&+\sum_{n=3}^{4}\mu\frac{n}{2}\left\{\hat{A}_n^*(2\hat{\alpha}_l)\hat{r}_l^{(n-2)/2}\cos(\frac{n-2}{2})\hat{\theta}_l\right.\\
&\left.+\hat{B}_n^*(t)(1+\hat{\alpha}_s^2)\hat{r}_s^{(n-2)/2}\cos(\frac{n-2}{2})\hat{\theta}_s\right\}
\end{aligned} \qquad (26)$$

Applying traction free boundary conditions on the crack surface, $\hat{A}_n^o(t)$, $\hat{B}_n^o(t)$, $\hat{A}_n^*(t)$ and $\hat{B}_n^*(t)$ can be obtained as

$$\hat{A}_n^o(t) = -\frac{2}{\mu_c\sqrt{2\pi}}\hat{B}_I(c,\dot{c},t)\hat{K}_n^o(t)$$
$$\hat{A}_n^*(t) = \frac{2}{\mu_c\sqrt{2\pi}}\hat{B}_{II}(c,\dot{c},t)\hat{K}_n^*(t)$$
$$\hat{B}_n^o(t) = -h_n^o(c,\dot{c},t)\hat{A}_n^o(t) \quad \hat{B}_n^*(t) = -h_n^*(c,\dot{c},t)\hat{A}_n^*(t) \quad (27)$$

where

$$\hat{B}_I(c,\dot{c},t) = \frac{(1+\hat{\alpha}_s^2)(1-\alpha_I^2)}{4\alpha_I\hat{\alpha}_s(1-\alpha_I^2)+(1+\alpha_s^2)[(1-\alpha_s^2)(1-\hat{\alpha}_I^2)-2(1-\alpha_I^2)]},$$
$$\hat{B}_{II}(c,\dot{c},t) = \frac{2\hat{\alpha}_s(1-\alpha_I^2)}{4\alpha_I\hat{\alpha}_s(1-\alpha_I^2)+(1+\alpha_s^2)[(1-\alpha_s^2)(1-\hat{\alpha}_I^2)-2(1-\alpha_I^2)]},$$
$$h_3^o(c,\dot{c},t) = h_4^*(c,\dot{c},t) = \frac{2\hat{\alpha}_I}{(1+\hat{\alpha}_s^2)}$$
$$h_3^*(c,\dot{c},t) = h_4^o(c,\dot{c},t) = \frac{2(1-\alpha_I^2)-(1-\alpha_s^2)(1-\hat{\alpha}_I^2)}{2\hat{\alpha}_s(1-\alpha_I^2)}$$

Substituting Eq. (27) into Eq. (26), applying $\hat{A}_n^o(t) = \eta_{n-2}^o A_{n-2}^o(t)/k_n^o(t)$ and $\hat{A}_n^*(t) = \eta_{n-2}^* A_{n-2}^*/k_n^*$, the stress fields σ_{ijn} can be obtained as Eq. (28)

$$\sigma_{xxn} = \sum_{n=3}^{4}\frac{nK_n^o(t)}{\sqrt{2\pi}}B_I(c)\exp(\varsigma x)\left\{\left[\frac{1-\alpha_s^2}{1-\alpha_I^2}(1-\hat{\alpha}_I^2)+2\hat{\alpha}_I^2\right]\hat{r}_I^{\frac{n-2}{2}}\times\cos(\frac{n-2}{2})\hat{\theta}_I - 2h_n^o\hat{\alpha}_s\hat{r}_s^{\frac{n-2}{2}}\cos(\frac{n-2}{2})\hat{\theta}_s\right\}$$
$$+\sum_{n=3}^{4}\frac{nK_n^*(t)}{\sqrt{2\pi}}B_{II}(c)\exp(\varsigma x)\left\{\left[\frac{1-\alpha_s^2}{1-\alpha_I^2}(1-\hat{\alpha}_I^2)+2\hat{\alpha}_I^2\right]\hat{r}_I^{\frac{n-2}{2}}\times\sin(\frac{n-2}{2})\hat{\theta}_I - 2h_n^*\hat{\alpha}_s\hat{r}_s^{\frac{n-2}{2}}\sin(\frac{n-2}{2})\hat{\theta}_s\right\}$$
$$\sigma_{yyn} = \sum_{n=3}^{4}\frac{nK_n^o(t)}{\sqrt{2\pi}}B_I(c)\exp(\varsigma x)\left\{\left[\frac{1-\alpha_s^2}{1-\alpha_I^2}(1-\hat{\alpha}_I^2)-2\right]\hat{r}_I^{\frac{n-2}{2}}\times\cos(\frac{n-2}{2})\hat{\theta}_I + 2h_n^o\hat{\alpha}_s\hat{r}_s^{\frac{n-2}{2}}\cos(\frac{n-2}{2})\hat{\theta}_s\right\}$$
$$+\sum_{n=3}^{4}\frac{nK_n^*(t)}{\sqrt{2\pi}}B_{II}(c)\exp(\varsigma x)\left\{\left[\frac{1-\alpha_s^2}{1-\alpha_I^2}(1-\hat{\alpha}_I^2)-2\right]\hat{r}_I^{\frac{n-2}{2}}\times\sin(\frac{n-2}{2})\hat{\theta}_I + 2h_n^*\hat{\alpha}_s\hat{r}_s^{\frac{n-2}{2}}\sin(\frac{n-2}{2})\hat{\theta}_s\right\}$$
$$\tau_{xyn} = \sum_{n=3}^{4}\frac{nK_n^o(t)}{\sqrt{2\pi}}B_I(c)\exp(\varsigma x)\times\left\{-2\hat{\alpha}_I\hat{r}_I^{\frac{n-2}{2}}\sin(\frac{n-2}{2})\hat{\theta}_I + (1+\hat{\alpha}_s^2)h_n^o\hat{r}_s^{\frac{n-2}{2}}\sin(\frac{n-2}{2})\hat{\theta}_s\right\}$$
$$+\sum_{n=3}^{4}\frac{nK_n^*(t)}{\sqrt{2\pi}}B_{II}(c)\exp(\varsigma x)\left\{2\hat{\alpha}_I\hat{r}_I^{\frac{n-2}{2}}\cos(\frac{n-2}{2})\hat{\theta}_I - (1+\hat{\alpha}_s^2)h_n^*\hat{r}_s^{\frac{n-2}{2}}\cos(\frac{n-2}{2})\hat{\theta}_s\right\} \quad (28)$$

where

$$K_3^o(t) = \eta_1^o K_I(t)/k_3^o, \quad K_4^o(t) = \eta_2^o K_2^o(t)/k_4^o,$$
$$K_3^*(t) = \eta_1^* K_{II}(t)/k_3^*, \quad K_4^*(t) = \eta_2^* K_2^*(t)/k_4^*,$$
$$\hat{r}_I = \sqrt{x^2+(\hat{\alpha}_I y)^2}, \quad \hat{r}_s = \sqrt{x^2+(\hat{\alpha}_s y)^2},$$
$$\hat{\theta}_I = \tan^{-1}[\hat{\alpha}_I y/x], \quad \hat{\theta}_s = \tan^{-1}[\hat{\alpha}_s y/x],$$

Substituting Eq. (25) into Eq.(23), the displacement fields can be obtained as

$$u_n = \sum_{n=3}^{4}\frac{K_n^o(t)B_I(c)}{\mu_o\exp(\varsigma a)}\sqrt{\frac{2}{\pi}}\times\left\{\hat{r}_I^{\frac{n}{2}}\cos(\frac{n}{2})\hat{\theta}_I - \hat{\alpha}_s h_n^o r_s^{\frac{n}{2}}\cos(\frac{n}{2})\hat{\theta}_s\right\}$$
$$+\sum_{n=3}^{4}\frac{K_n^*(t)B_{II}(c)}{\mu_o\exp(ax)}\sqrt{\frac{2}{\pi}}\times\left\{\hat{r}_I^{\frac{n}{2}}\sin(\frac{n}{2})\hat{\theta}_I - \hat{\alpha}_s h_n^*\hat{r}_s^{\frac{n}{2}}\sin(\frac{n}{2})\hat{\theta}_s\right\}$$
$$v_n = \sum_{n=3}^{4}\frac{K_n^o(t)B_I(c)}{\mu_o\exp(\varsigma a)}\sqrt{\frac{2}{\pi}}\times\left\{-\hat{\alpha}_I\hat{r}_I^{\frac{n}{2}}\sin(\frac{n}{2})\hat{\theta}_I + h_3^o\hat{r}_s^{\frac{n}{2}}\sin(\frac{n}{2})\hat{\theta}_s\right\}$$
$$+\sum_{n=3}^{4}\frac{K_n^*(t)B_{II}(c)}{\mu_o\exp(\varsigma a)}\sqrt{\frac{2}{\pi}}\times\left\{\hat{\alpha}_I\hat{r}_I^{\frac{n}{2}}\cos(\frac{n}{2})\hat{\theta}_I - h_n^*\hat{r}_s^{\frac{n}{2}}\cos(\frac{n}{2})\hat{\theta}_s\right\} \quad (29)$$

Finally, the fields for a propagating transient crack in FGM under inplane loading, σ_{ij} and $u(v)$ are given in Eq. (30)

$$\sigma_{ij} = \sum_{n=1}^{4}\sigma_{ijn}, \quad u(v) = \sum_{n=1}^{4}u_n(v_n) \quad (30)$$

The structure of the transient fields of $n = 3,\ 4$ is similar to that of the steady fields of $n = 1,\ 2$ because the higher order terms are obtained by transforming the partial differential equation of the dynamic equilibrium into Laplace's equation whose solution has harmonic function. Especially, the higher orders terms of $n \geq 3$ are affected by terms of the nonhomogeneity parameter ς, crack tip acceleration $\dot{c}$ and the rate of change of stress intensity factor $(\dot{K})$. When ς are zero, the equations reduce to the fields for a transiently propagating crack in isotropic materials [15]. This analytical method and the results are different from those of previous studies [13, 14]. In previous studies [13, 14], the higher order terms in the fields are very complex because they were obtained not from Laplace's equilibrium equation but the general partial differential equation. In addition, some terms in the fields approach infinity as a crack speed approaches zero as pointed out by Chalivendra and Shukla [14] and this irregularity occurs for $c < 0.3c_s$. Therefore, they suggested that the fields should be applied by a remedial approximation for $c < 0.3c_s$. However, the fields in this study do not have any irregularity and can be applied from a stationary crack speed to Rayleigh wave speed.

3. Discussion on solutions

3.1 Effect of transient factors on stress fields

In order to investigate the effects of transients $\dot{c}$, $\dot{K}$ on stress components, transient fields of Eq. (30) for mode I and II loading are used. The coefficients $(n = 1,\ 3)$ related to stress intensity factors were considered. To analyze the exact stress and displacement components, the reasonable selection of $k_3^{o(*)}$ in Eq. (20) and $K_3^{o(*)}$ in Eq. (30) is very important. Various values of $k_3^{o(*)}$ and $K_3^{o(*)}$ can be selected, however, two conditions are demanded.

First, when a crack propagates with steady state ($\dot{c} = \dot{K} = 0$), the normalized stress components $(\sigma_{yy})_{\theta=0^o}/\sigma_I^+$ (see Fig. 4) and $(\tau_{xy})_{\theta=0^o}/\sigma_{II}^+$ (see Fig. 8) at $r \to 0$ must be constant at any crack velocity [10, 15-17]. Second, the higher order normalized stress components σ_{yy3}/σ_I^+ and τ_{xy3}/σ_{II}^+ in Eq. (30) must have small values at $r \to 0(\theta = 0^o)$ when $\dot{c}$ and $\dot{K}$ are zero. That is, $\left|\sigma_{yy}(=\sigma_{yy1}+\sigma_{yy3})\right|/\sigma_{yy1} \approx 1$ and $\left|\tau_{xy}(=\tau_{yy1}+\tau_{xy3})\right|/\tau_{xy1} \approx 1$ when $r \to 0(\theta = 0^o)$ and $\dot{c} = \dot{K}(t) = 0$. In this study, when $\dot{c} = \dot{K} = 0$, $\left|\sigma_{yy3}/\sigma_{yy1}\right| < 0.02$ for mode I, $\left|\tau_{xy3}/\tau_{xy1}\right| < 0.02$ for node II, where $r = 0.01$m. These values of $k_3^{o(*)}$ and $K_3^{o(*)}$ selected in this study satisfy the above two conditions. The stress components were evaluated as a function of the angular position (θ) at radial location $r = 0.01$m for stationary and propagating cracks. The stress intensity factors $K_I(t) = K_{II}(t) =$ 1.0MPa(m)$^{1/2}$. Physical properties $\mu(X) = 1.316e^{\varsigma X}$ (GPa), $\rho(X) = 1200e^{\varsigma X}$ (kg/m^3), ς = 4/m or (–4/m), $\nu = 0.38$ and material fringe constant f_σ = 15 (kN/m-fringe).

Table 1 shows the values of $k_3^{o(*)}$ and $K_3^{o(*)}$ used for analyzing stress components of a transiently propagating crack. When $M = 0.02$, the values of k_3^o and k_3^* are very high. However, the low values of k_3^o and k_3^* can also be used if two conditions previously mentioned are satisfied.

Fig. 2 shows the stress component in the vicinity of the crack tip propagating at acceleration, deceleration or constant velocity in functionally graded materials with an exponential variation of physical properties.

Fig. 3 shows the normalized stress σ_{xx}/σ_I^+ with variation of $\dot{K}_I$ at crack tip when crack is a stationary ($M = 0.02$) and propagates at $M = 0.7$ under mode I loading. Where $k_3^o = 10^5$m

Table 1. The coefficients used for analyzing stress components of a transiently propagating crack.

Figs	Mode I			Mode II	
	M	$\dot{c}$(m/s^2), $\dot{K}_I$(MPa$\sqrt{\text{m}}$/s)	k_3^o(m), K_3^o(MPa/$\sqrt{\text{m}}$)	$\dot{c}$(m/s^2), $\dot{K}_{II}$(MPa$\sqrt{\text{m}}$/s)	k_3^*(m), K_3^*(MPa/$\sqrt{\text{m}}$)
Figs 3~8	0.02	$\dot{c} = 0$ $\dot{K}_I(t) = 0 \sim 10^2$	$k_3^* = 10^5$m $K_3^o = K_I/k_3^o$	$\dot{c} = 0$ $\dot{K}_{II} = 0 \sim 10^2$	$k_3^o = 10^5$m $K_3^* = 10^{-4}K_{II}/k_3^*$
	0.7	$\dot{c} = 0$ $\dot{K}_I = 0 \sim 10^3$	$k_3^o = 0.9$m $K_3^o = K_I/k_3^o$	$\dot{c} = 0$ $\dot{K}_{II} = 0 \sim 10^3$	$k_3^* = 0.9$m $K_3^* = K_I/k_3^*$
Figs 9~14	0.2	$\dot{c} = -2\times10^7 \sim 2\times10^7$ $\dot{K}_I = 10^5$	$k_3^o = 0.02$m $K_3^o = 10^{-2}K_I/k_3^o$	$\dot{c} = -2\times10^7 \sim 2\times10^7$ $\dot{K}_{II} = 10^5$	$k_3^* = 0.02$m $K_3^* = 10^{-2}K_{II}/k_3^*$

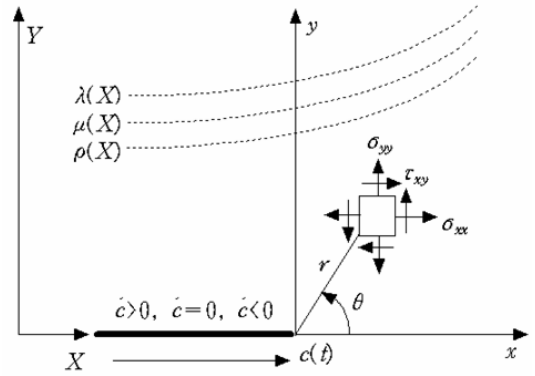

Fig. 2. Stress components in the vicinity of the propagating crack tip.

for stationary crack ($M = 0.02$) and $k_3^o = 0.9\text{m}$ for propagating crack with $M = 0.7$. $\dot{K}_I$ varies in the range $0 \sim 100\text{MPa(m)}^{1/2}/\text{s}$ for stationary crack and $0 \sim 1000\text{MPa(m)}^{1/2}/\text{s}$ for propagating crack with $M = 0.7$. In Fig. 3, as $\dot{K}_I$ increases, the normalized stress σ_{xx}/σ_I^+ decreases and the effect of variation of $\dot{K}_I$ on σ_{xx} is great in $60^o < |\theta| < 120^o$ when the crack is static and near $\theta = 0^o$ and 90^o when crack is propagating at $M = 0.7$. Even if the value of K_3^o and the variation of $\dot{K}_I$ is greater when $M = 0.7$ than when $M = 0.02$ (see Table 1), the variation of stress σ_{xx} is greater when crack is static than when crack propagates. Thus, the effect of $\dot{K}_I$ on stress σ_{xx} is greater when crack velocity is slow than fast.

Fig. 4 shows the normalized stress σ_{yy}/σ_I^+ with variation of $\dot{K}_I$ at crack tip when crack is a stationary ($M = 0.02$) and propagates at $M = 0.7$ under the same conditions as Fig. 3. In steady state ($\dot{c} = \dot{K}(t) = 0$), normalized stress component $\sigma_{yy}(\theta = 0^o)/\sigma_I^+$ when $M = 0.02$ is the same as that when $M = 0.7$. This point will have to be considered when the values of k_3^o and K_3^o are selected. As known in Fig. 4, as $\dot{K}_I$ increases, the normalized stress σ_{yy}/σ_I^+ decreases and the effect of variation of $\dot{K}_I$ on σ_{yy} is great in $20^o < |\theta| < 150^o$ when $M = 0.02$ and $|\theta| < 80^o$ when $M = 0.7$. The effect of $\dot{K}_I$ on stress σ_{yy} is greater when the crack is static than when the crack propagates.

Fig. 5 shows the normalized stress τ_{xy}/σ_I^+ with variation of $\dot{K}_I$ at crack tip when crack is a stationary and propagates at $M = 0.7$ under the same condition as Fig. 3. As $\dot{K}_I$ increases, the normalized stress τ_{xy}/σ_I^+ increases in $0^o < \theta < 180^o$ and decreases in $-180^o < \theta < 0^o$ for stationary crack

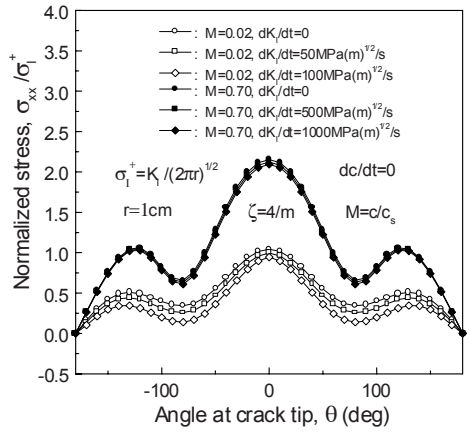

Fig. 3. Normalized stress σ_{xx}/σ_I^+ for variation of $\dot{K}_I(t)$ under $K_I(t) = 1.0\text{MPa(m)}^{1/2}$.

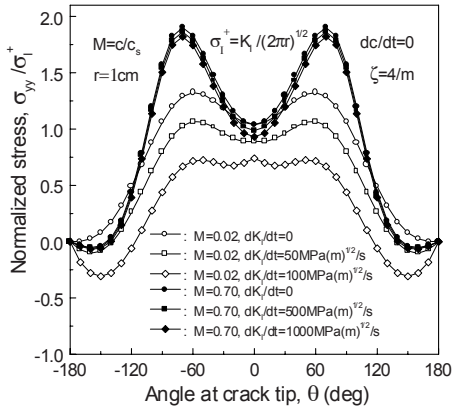

Fig. 4. Normalized stress σ_{yy}/σ_I^+ for variation of $\dot{K}_I(t)$ under $K_I(t) = 1.0\text{MPa(m)}^{1/2}$.

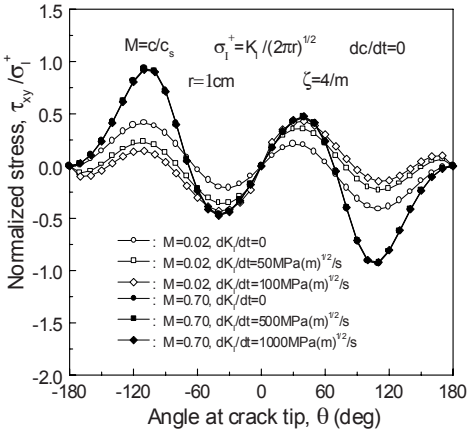

Fig. 5. Normalized stress τ_{xy}/σ_I^+ for variation of $\dot{K}_I(t)$ under $K_I(t) = 1.0\text{MPa(m)}^{1/2}$.

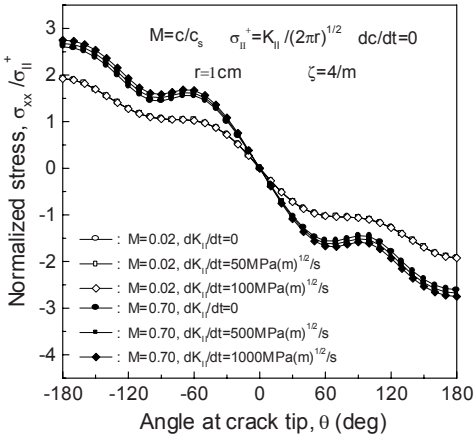

Fig. 6. Normalized stress $\sigma_{xx}/\sigma_{II}^{+}$ for variation of $\dot{K}_{II}(t)$ under $K_{II}(t)=1.0\text{MPa(m)}^{1/2}$.

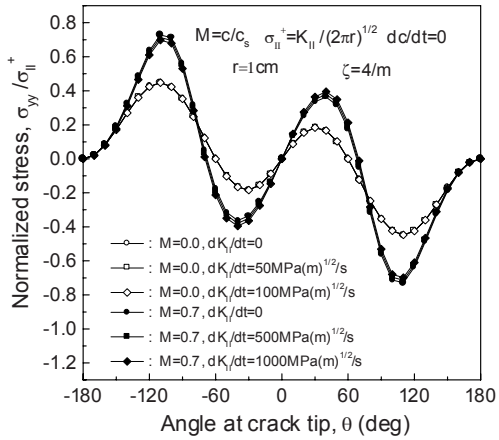

Fig. 7. Normalized stress $\sigma_{yy}/\sigma_{II}^{+}$ for variation of $\dot{K}_{II}(t)$ under $K_{II}(t)=1.0\text{MPa(m)}^{1/2}$.

and the effect of variation of $\dot{K}_I$ on τ_{xy} is great in $20^o<|\theta|<160^o$. The maximum values of absolute $|\tau_{xy}/\sigma_I^{+}|$, which occur at $\theta=\pm 110^o$, decrease as $\dot{K}_I$ increases. When the crack propagates at $M=0.7$, the effect of $\dot{K}_I$ on τ_{xy} is less than that on σ_{xx}/σ_I^{+} and σ_{yy}/σ_I^{+}.

Figs. 6-8 show the normalized stresses $\sigma_{xx}/\sigma_{II}^{+}$, $\sigma_{yy}/\sigma_{II}^{+}$ and $\tau_{xy}/\sigma_{II}^{+}$ with variation of $\dot{K}_{II}$ at crack tip when crack is a stationary ($M=0.02$) and propagates at $M=0.7$ under mode II loading. Where $k_3^{*}=10^5\text{m}$ for stationary crack ($M=0.02$) and $k_3^{*}=0.9\text{m}$ for propagating crack ($M=0.7$). As known in figures, in steady state $\dot{c}=\dot{K}(t)=0$, $\tau_{xy}(\theta=0^o)/\sigma_{II}^{+}$ when $M=0.02$ is the same as that when $M=0.7$. As pointed out previously, this fact

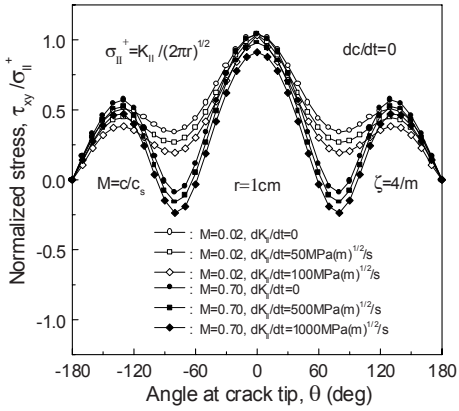

Fig. 8. Normalized stress $\tau_{xy}/\sigma_{II}^{+}$ for variation of $\dot{K}_{II}(t)$ under $K_{II}(t)=1.0\text{MPa(m)}^{1/2}$.

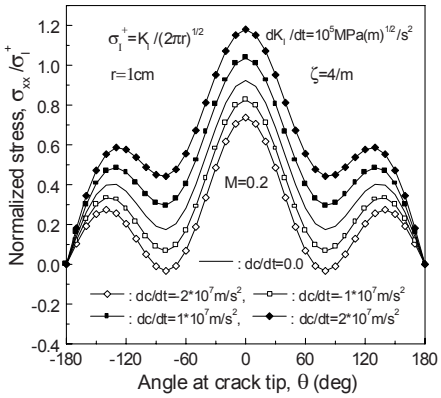

Fig. 9. Normalized stress σ_{xx}/σ_I^{+} for variation $\dot{c}$ under $K_I(t)=1.0\text{MPa(m)}^{1/2}$.

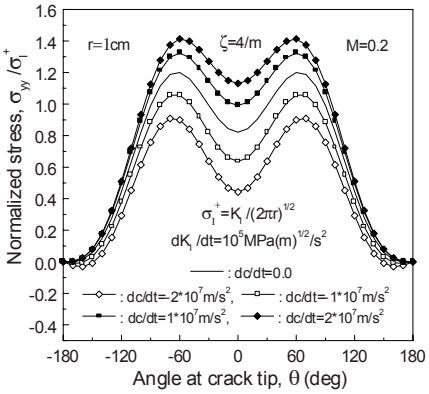

Fig. 10. Normalized stress σ_{yy}/σ_I^{+} for variation $\dot{c}$ under $K_I(t)=1.0\text{MPa(m)}^{1/2}$.

will have to be considered to select the values of k_3^{*} and K_3^{*}. The effect of variation of $\dot{K}_{II}$ on $\tau_{xy}/\sigma_{II}^{+}$ is great; however, that on $\sigma_{xx}/\sigma_{II}^{+}$ and $\sigma_{yy}/\sigma_{II}^{+}$ is

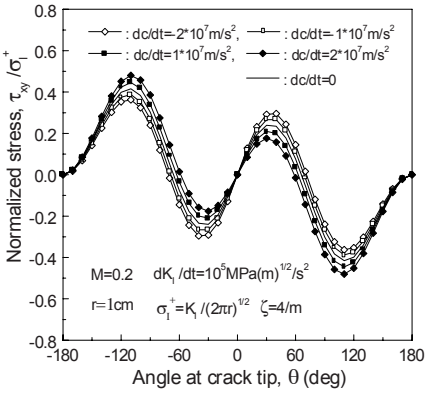

Fig. 11. Normalized stress τ_{xy}/σ_I^+ for variation $\dot{c}$ under $K_I(t)=1.0\text{MPa(m)}^{1/2}$.

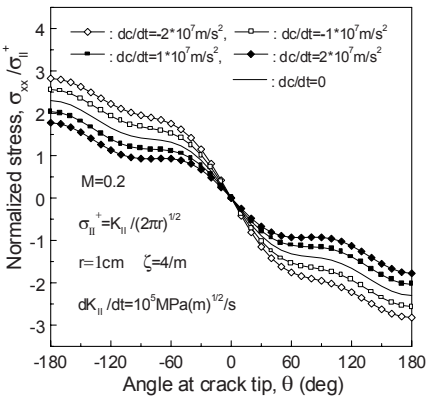

Fig. 12. Normalized stress $\sigma_{xx}/\sigma_{II}^+$ for variation $\dot{c}$ under $K_{II}(t)=1.0\text{MPa(m)}^{1/2}$.

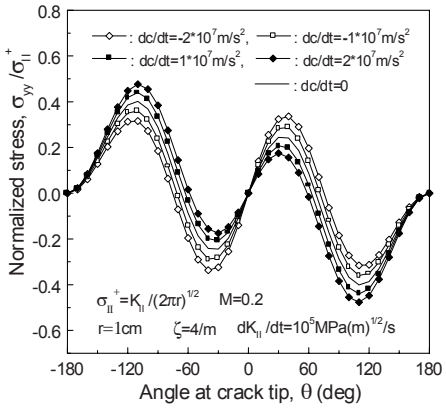

Fig. 13. Normalized stress $\sigma_{yy}/\sigma_{II}^+$ for variation $\dot{c}$ under $K_{II}(t)=1.0\text{MPa(m)}^{1/2}$.

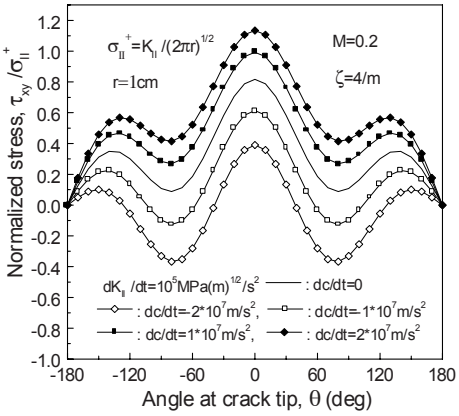

Fig. 14. Normalized stress τ_{xy}/σ_{II}^+ for variation. $\dot{c}$ under $K_{II}(t)=1.0\text{MPa(m)}^{1/2}$.

little. The effect of variation of $\dot{K}_{II}$ on τ_{xy}/σ_{II}^+ is great in $|\theta|<160^o$. It seems that the effect of variation of $\dot{K}_{II}$ on $\sigma_{xx}/\sigma_{II}^+$ is greater when $M=0.7$ than when $M=0.02$; however, if the variation of $\dot{K}_{II}$ is from 0 to $100\text{MPa(m)}^{1/2}$/s as case of $M=0.02$, the effect of $\dot{K}_{II}$ on $\sigma_{xx}/\sigma_{II}^+$ is very little. The effect of $\dot{K}_{II}$ on variation of stresses is also higher when crack velocity is slow than fast.

From Fig. 3 to 8, as the change rate of stress intensity factor for time ($\dot{K}_I$) increases, the stresses σ_{xx}/σ_I^+, σ_{yy}/σ_I^+ and τ_{xy}/σ_{II}^+, which are not zero at $\theta=0^o$, decrease but $\sigma_{xx}/\sigma_{II}^+$ increases. τ_{xy}/σ_I^+ and $\sigma_{yy}/\sigma_{II}^+$, which are zero at $\theta=0^o$, increase or decrease along crack tip θ. However, the maximum values of absolute $|\tau_{xy}/\sigma_I^+|$ and $|\sigma_{yy}/\sigma_{II}^+|$, which occur at $\theta=\pm110^o$, decrease as $\dot{K}_I$ and $\dot{K}_{II}$ increases. The effect of $\dot{K}_I$ on variation of stresses is higher when crack velocity is slow than fast.

Fig. 9 shows the normalized stress σ_{xx}/σ_I^+ with variation of $\dot{c}$ at crack tip when the crack propagates at $M=0.2$ under mode I loading. The acceleration will occur greatly at crack initiation even if the crack speed is slow. After accelerating, the crack will propagate at almost constant velocity and will be stopping (deceleration). Thus, the low crack velocity $M=0.2$ is selected in other to evaluate the effect of acceleration or deceleration on stress components. The range of $\dot{c}$ is $-2\times10^7 \sim 2\times10^7\text{m/s}^2$ under $\dot{K}_I=10^5\text{MPa(m)}^{1/2}$/s. When the crack acceleration ($\dot{c}>0$) increases, the normalized σ_{xx}/σ_I^+ at crack tip increases. When the crack deceleration ($\dot{c}<0$) increases, σ_{xx}/σ_I^+ decreases.

The effect of $\dot{c}$ on σ_{xx} is great in $|\theta| < 140^o$ and greatest at $\theta = 0^o$. Compared with Fig. 9(a) and (b), the higher the transients ($\dot{c}$, $\dot{K}_I(t)$), the greater the variation of σ_{xx}/σ_I^+.

Fig. 10 shows the normalized stress σ_{yy}/σ_I^+ with variation of $\dot{c}$ at crack tip when the crack propagates at $M = 0.2$ under the same condition as Fig. 9. As the crack propagates at acceleration ($\dot{c} > 0$), the normalized σ_{yy}/σ_I^+ increases, as the crack propagates at deceleration ($\dot{c} < 0$), σ_{yy}/σ_I^+ decreases. The effect of $\dot{c}$ on σ_{yy} is great in $|\theta| < 100^o$ and greatest at $\theta = 0^o$. The higher the transients ($\dot{c}$, $\dot{K}$), the greater the variation of σ_{yy}/σ_I^+.

Fig. 11 shows the normalized stress τ_{xy}/σ_I^+ with variation of $\dot{c}$ at crack tip when the crack propagates at $M = 0.2$ under the same conditions as Fig. 9. τ_{xy}/σ_I^+ increases in $0^o < \theta < 180^o$ and decreases in $-180^o < \theta < 0^o$ when the crack is accelerating. However, maximum values of absolute $|\tau_{xy}/\sigma_I^+|$, which occur at $|\theta| = 110^o$, increase as the acceleration increases.

Fig. 12 shows the normalized stress $\sigma_{xx}/\sigma_{II}^+$ with variation of $\dot{c}$ at crack tip when the crack propagates at $M = 0.2$ under mode II loading. The range of $\dot{c} = -2\times10^7 \sim 2\times10^7\,\mathrm{m/s^2}$ under $\dot{K}_I = 10^5\,\mathrm{MPa(m)^{1/2}/s}$. The normalized $|\sigma_{xx}/\sigma_{II}^+|$ is greater when the crack propagates at deceleration than acceleration. The effect of $\dot{c}$ on $\sigma_{xx}/\sigma_{II}^+$ is great in $|\theta| > 30^o$ and greatest at crack face which is $|\theta| = 180^o$.

Fig. 13 shows the normalized stress $\sigma_{yy}/\sigma_{II}^+$ with variation of $\dot{c}$ at crack tip when the crack propagates at $M = 0.2$ under the same condition as Fig. 12. $\sigma_{yy}/\sigma_{II}^+$ increases in $0^o < \theta < 180^o$ and decreases in $-180^o < \theta < 0^o$ when crack is accelerating. However, maximum values of absolute $|\sigma_{yy}/\sigma_{II}^+|$, which occur at $|\theta| = 110^o$, increase as the acceleration increases.

Fig. 14 shows the normalized stress τ_{xy}/σ_{II}^+ with variation of $\dot{c}$ at crack tip when the crack propagates at $M = 0.2$ under the same condition as Fig. 12. When the crack propagates at acceleration, the normalized $|\tau_{xy}/\sigma_{II}^+|$ increases; when the crack propagates at deceleration, it decreases. The effect of $\dot{c}$ on τ_{xy}/σ_{II}^+ is great in $|\theta| < 150^o$ and greatest in the $|\theta| = 80^o$.

From Figs. 9 to 14, one can know that the stresses of σ_{xx}/σ_I^+, σ_{yy}/σ_I^+ and τ_{xy}/σ_{II}^+ which are not zero at $\theta = 0^o$ increase as the crack propagates at acceleration and decrease at deceleration. The stresses of τ_{xy}/σ_I^+ and $\sigma_{yy}/\sigma_{II}^+$ which are zero at $\theta = 0^o$, increase in $0^o < \theta < 180^o$ and decrease in $-180^o < \theta < 0^o$ when the crack is accelerating. However, the maximum values of absolute $|\tau_{xy}/\sigma_I^+|$ and $|\sigma_{yy}/\sigma_{II}^+|$ increase as crack acceleration increases. $|\sigma_{xx}/\sigma_{II}^+|$ decreases as the crack propagates at acceleration.

3.2 Isochromatics for a transiently propagating crack

In order to investigate the effects of the transient terms on a dynamic fracture, contours of constant maximum shear stress (isochromatics) are generated for the opening and shear mode using the terms $n = 1$ and 3 in Eq. (30). The material thickness (h) used in generating the contours is 9.5 mm. Isochromatics at each point around crack tip are generated by the stress optic law (Eq. 31) combined with stress fields.

$$\sqrt{(\sigma_{xx} - \sigma_{yy})^2 + 4\tau_{xy}^2} = \frac{Nf_\sigma}{h} \tag{31}$$

where N is the fringe order, h the plate thickness and f_σ the material fringe constant.

Fig. 15 shows the effect of the rate of change of mode I stress intensity factor $\dot{K}_I$ for a stationary crack tip ($M = 0.02$) under $\dot{c} = 0$, $\varsigma = 4/\mathrm{m}$, $k_3^o = 0.005\mathrm{m}$ and $K_3^o(t) = 0.05K_I(t)/\mathrm{m}$. If $k_3^o = 10^5\,\mathrm{m}$ and $K_3^o(t) = 10^{-5}K_I(t)/\mathrm{m}$ are applied, the isochromatics are very sensitive on the variation of $\dot{K}_I$ because the value of k_3^o is very high. Even if $\dot{K}_I = 0$, the contours, due to nonhomogeneity away from crack tip, tilt away the crack face. Generally, when $\varsigma > 0$ (modulus increases ahead of the crack), the fringes tilt forward whereas for $\varsigma < 0$, the fringes tilt backward. As $\dot{K}_I$ increases, the fringes tilt more for-ward around the crack tip, and the size of the fringes decreases. This variation occurs largely when the rate of change of the stress intensity factor is high.

Fig. 16 shows the effect of crack tip acceleration $\dot{c}$ for a crack tip propagating with M=0.2 under $\dot{K}_I = 10^5\,\mathrm{MPa(m)^{1/2}/s}$, $\varsigma = 4/\mathrm{m}$, $k_3^o = 0.02\mathrm{m}$ and $K_3^o(t) = 0.5K_I(t)/\mathrm{m}$. When the rate of change of velocity compared to crack tip speed is too high, Eq. (20) cannot be applied. However, when a small value of k_3^o is used in Eq. (20), a higher $\dot{c}$ can be applied in Eq. (20). It can be seen in Fig. 16 that the fringes tilt backward around the crack tip with

increasing crack tip acceleration. This variation also occurs largely at a high rate of change of velocity. Generally, the isochromatic fringes at fast propagating crack tip under mode I loading tilt more towards the crack face (backward) compared to those for a stationary crack. The phenomenon also occurs when the crack tip acceleration $\dot{c}$ increases.

Fig. 17 shows the effect of crack tip acceleration $\dot{c}$ for a crack tip propagating with M=0.5 for $\varsigma = 4/\mathrm{m}$ under lower transients than those in Fig. 16. It seems that the transients will occur greatly at crack initiation when crack velocity is slow. The transients at crack velocity of M=0.5 will be lower than those at crack initiation. Thus, the transients are applied lower values than those in Fig. 16. $\dot{K}_I = 10^3\,\mathrm{MPa(m)^{1/2}/s}$ and the range of acceleration is $0 \sim 3\times10^6\,\mathrm{m/s^2}$.

When $k_3^o = 0.5\mathrm{m}$, Eq. (20) can be applied enough for the range of $\dot{c} = 0 \sim 3\times10^6\,\mathrm{m/s^2}$. $K_3^o(t)$ is $2K_I(t)/\mathrm{m}$, which is higher than $0.5K_I(t)/\mathrm{m}$ in Fig. 16. If $K_3^o(t)$ is $0.5K_I(t)/\mathrm{m}$ as in Fig.17, the effect of acceleration on isochromatics is little. Anyway, the fringes tilt backward around the crack tip with increasing crack tip acceleration. Compared with Fig. 16, the higher the acceleration is, the more tilted the fringe at crack tip is.

Fig. 18 shows the effect of crack tip acceleration $\dot{c}$ for a crack tip propagating with M=0.5 under, $\dot{K}_I = 10^3\,\mathrm{MPa(m)^{1/2}/s}$, $\varsigma = -4/\mathrm{m}$, $k_3^o = -0.5\mathrm{m}$ and $K_3^o(t) = -2K_I(t)/\mathrm{m}$. If $k_3^o << 1$, though $\varsigma < 0$, k_3^o of positive number can be applied in Eq. (20), and then $K_3^o(t) > 0$. Unlike $\varsigma = 4/\mathrm{m}$ in Fig. 17, it can be also observed that the fringes also tilt backward almost constantly, but their sizes increase around the crack tip when the crack tip acceleration increases. The above results indicate that the isochromatic fringes, due to high negative ς, tilt backward too much.

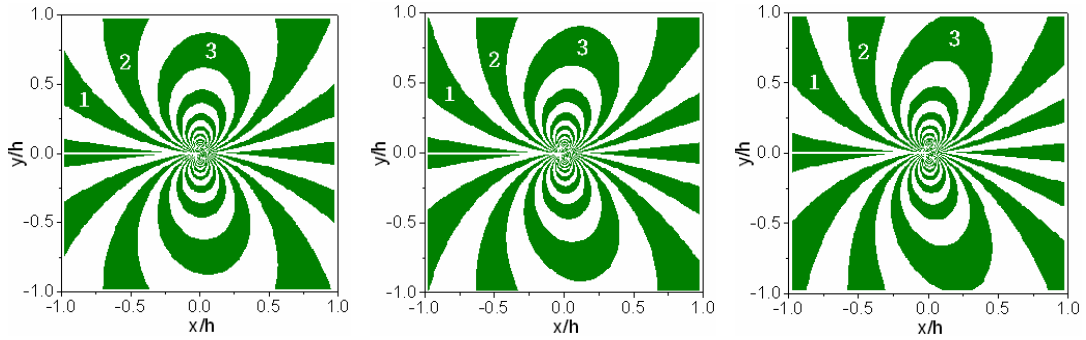

(a) $\dot{K}_I(t) = 0$ (b) $\dot{K}_I(t) = 10^5\,\mathrm{MPa(m)^{1/2}/s}$ (c) $\dot{K}_I(t) = 5\times10^5\,\mathrm{MPa(m)^{1/2}/s}$

Fig. 15. Effect of rate of change of mode-I SIF for a stationary crack tip (M=0.02) under $\dot{c} = 0$, $K_I(t) = 1.0\,\mathrm{MPa(m)^{1/2}}$, $\varsigma = 4/\mathrm{m}$, $k_3^0 = 0.005\,\mathrm{m}$ and $K_3^0(t) = 0.05K_I(t)/\mathrm{m}$.

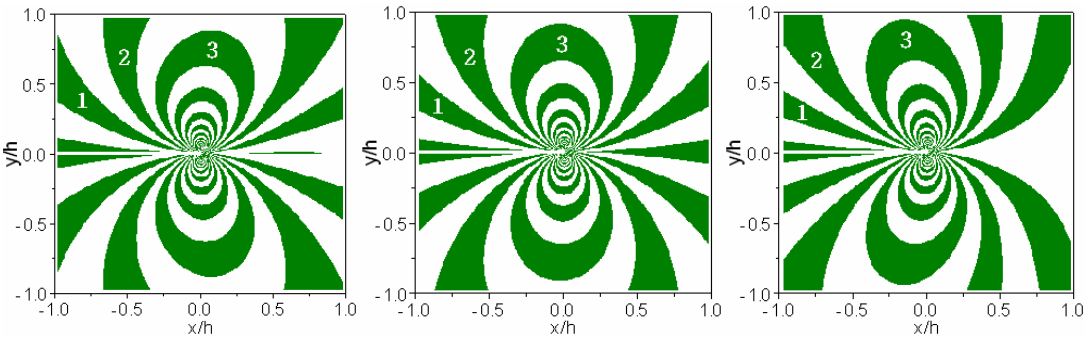

(a) $\dot{c} = 0$ (b) $\dot{c} = 2\times10^7\,\mathrm{m/s^2}$ (c) $\dot{c} = 3\times10^7\,\mathrm{m/s^2}$

Fig. 16. Effect of crack tip acceleration for a crack propagating with M=0.2 under $K_I(t) = 1.0\,\mathrm{MPa(m)^{1/2}}$, $\dot{K}_I(t) = 10^5\,\mathrm{MPa(m)^{1/2}/s}$, $\varsigma = 4/\mathrm{m}$, $k_3^0 = 0.02\,\mathrm{m}$ and $K_3^0(t) = 0.5K_I(t)/\mathrm{m}$.

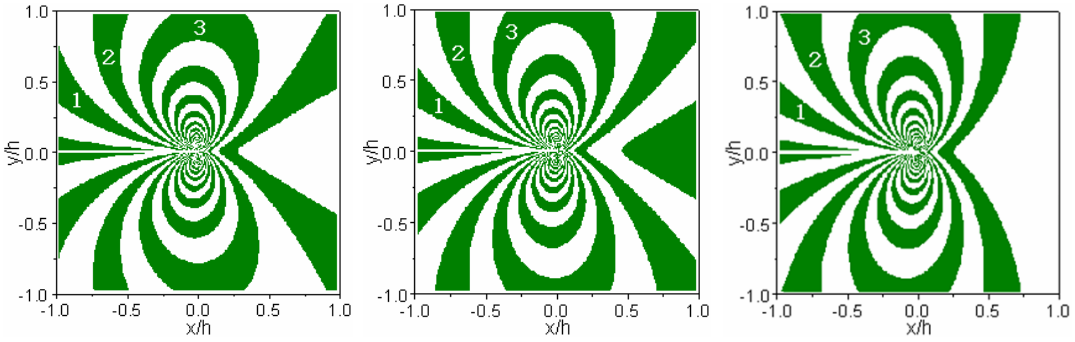

(a) $\dot{c}=0$ (b) $\dot{c}=2\times10^6$ m/s^2 (c) $\dot{c}=3\times10^6$ m/s^2

Fig. 17. Effect of crack tip acceleration for a crack propagating with M=0.5 under $K_I(t)=1.0\,\mathrm{MPa(m)}^{1/2}$, $\dot{K}_I(t)=10^3\,\mathrm{MPa(m)}^{1/2}/\mathrm{s}$, $\varsigma=4/\mathrm{m}$, $k_3^0=0.5\,\mathrm{m}$ and $K_3^0(t)=2K_I(t)/\mathrm{m}$.

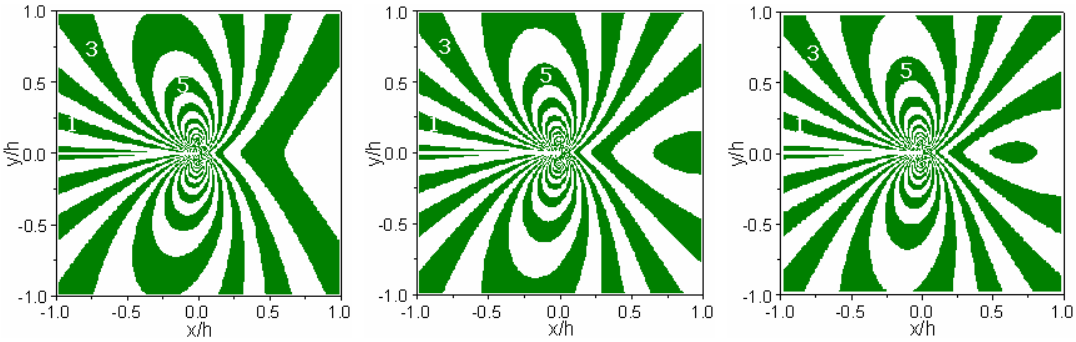

(a) $\dot{c}=0$ (b) $\dot{c}=2\times10^6$ m/s^2 (c) $\dot{c}=3\times10^6$ m/s^2

Fig. 18. Effect of crack tip acceleration for a crack propagating with M=0.5 under $K_I(t)=1.0\,\mathrm{MPa(m)}^{1/2}$, $\dot{K}_I(t)=10^3\,\mathrm{MPa(m)}^{1/2}/\mathrm{s}$, $\varsigma=-4/\mathrm{m}$, $k_3^0=-0.5\,\mathrm{m}$ and $K_3^0(t)=-2K_I(t)/\mathrm{m}$.

Thus, even if the acceleration increases, the tilts are almost constant, only the size is increased.

From Figs. 15 to 18, one can knows that the isochromatics are affected by crack tip speed c, crack tip acceleration $\dot{c}$ and the rate of change of the dynamic stress intensity factor $\dot{K}_I$. The isochromatics of mode I tilt backward around the crack tip as $\dot{c}$ increases and tilt forward around the crack tip as $\dot{K}_I$ increases. Generally, the isochromatics of mode I around crack tip obtained by the fields [10] of steady state crack propagation tilt more backward as a crack tip speed increases. It seems that the behavior occurs due to the increase of crack tip speed, that is, the crack tip acceleration. Thus, it is natural that the isochromatics of mode I obtained by transient fields should tilt more backward around the crack tip as $\dot{c}$ increases. However, Shukla and Jain's [13] results are the opposite of the present ones. Rosakis et al. [12] obtained the higher order asymptotic individual stress components near the tip of a non-uniformly propagating mode I crack for homogeneous material. Under the value of low $\dot{c}$ and $\dot{K}_I$, when we generate the contours for constant maximum shear stress of mode I state using their stress fields, the effects of $\dot{c}$ and $\dot{K}_I$ on constant maximum shear stress are the same as those in this study. However, under the value of high $\dot{c}$ and $\dot{K}_I$ used in Figs. 15~18, the maximum shear stress at the remote area is much higher than that at the crack tip. Actually, the stress at the crack tip must be much higher than that at any other area.

4. Conclusions

Using the stress components, effects of transients on stress components are studied. In addition, the contours of constant maximum shear stress (isochromatics) around the propagating crack are generated for crack speeds, accelerations, rates of change of stress

intensity factors and nonhomogeneity. The results are as follows.

(1) Effect of the change rate of stress intensity factor on stress components; As the change rate of stress intensity factors ($\dot{K}_I$, $\dot{K}_{II}$) increases, the stresses σ_{xx}/σ_I^+ , σ_{yy}/σ_I^+ and τ_{xy}/σ_{II}^+, which are not zero at $\theta = 0^o$, decreases but $\sigma_{xx}/\sigma_{II}^+$ increases. τ_{xy}/σ_I^+ and $\sigma_{yy}/\sigma_{II}^+$, which are zero at $\theta = 0^o$, increase or decrease along crack tip θ. However, the maximum values of absolute $\left|\tau_{xy}/\sigma_I^+\right|$ and $\left|\sigma_{yy}/\sigma_{II}^+\right|$, which occur at $\theta = \pm 110^o$, decrease as $\dot{K}_I$ and $\dot{K}_{II}$ increases. The effect of $\dot{K}_I$ on variation of stresses is higher when crack velocity is slow than fast.

(2) Effect of the change rate of crack velocity on stress components; As the crack acceleration $\dot{c}$ increases, the absolute stresses σ_{xx}/σ_I^+ , σ_{yy}/σ_I^+ and τ_{xy}/σ_{II}^+ increase. τ_{xy}/σ_I^+ and $\sigma_{yy}/\sigma_{II}^+$ increase or decrease along crack tip θ . However, the maximum values of absolute stresses of $\left|\tau_{xy}/\sigma_I^+\right|$ and $\left|\sigma_{yy}/\sigma_{II}^+\right|$ increase as crack acceleration $\dot{c}$ increases. $\sigma_{xx}/\sigma_{II}^+$ decreases as the crack propagates at acceleration. From (1) and (2), effects between $\dot{K}_{I(II)}$ and $\dot{c}$ on stress components are opposite to each other.

(3) The isochromatic fringes of mode I tilt backward around the crack tip with increase of crack tip acceleration $\dot{c}$ and tilt forward around the crack tip with increase of the rate of change of the dynamic mode I stress intensity factor ($\dot{K}_I$). These results are the opposite of Shukla & Jain's [13].

References

[1] C. Atkinson and R. D. List, Steady state crack propagation into media with spatially varying elastic properties. Int. J. Engng. Sci. 16 (1978)717-730.

[2] X. D. Wang and S. A. Meguid, On the dynamic crack propagation in an interface with spatially varying elastic properties. Int. J. Fract. 69 (1) (1994) 87-99.

[3] L. Y. Jiang and X. D. Wang, On the dynamic crack propagation in an interphase with spatially varying elastic properties under inplane loading. Int. J. Fract. 114 (3) (2002) 225-244.

[4] L. Ma, L. Z. Wu, Z. G. Zhou and T. Zeng, Crack propagating in a functionally graded strip under the plane loading. Int. J. Fract. 126 (1) (2004) 39-55.

[5] Z. Cheng and Z. Zhong, Analysis of moving crack in a functionally graded strip between two homogeneous layers. International Journal of Mechanical Science 49 (9) (2007) 1038-1046.

[6] C. -E. Rousseau and H. V. Tippur, Dynamic frac-ture of compositionally graded materials with cracks along the elastic gradient experiments and analysis. Mechanics of Materials. 33 (2001) 403-421.

[7] M. S. Kirugulige, R. Kitey and H. V. Tippur, Dynamic fracture behavior of model sandwich structures with functionally graded core: a feasibility study, Composites Science and Technology, 65(7-8) (2005) 1052-1068.

[8] X. F. Yao, S. L. Xu and H. Y. Yeh, Caustics analysis of the crack initiation and propagation of graded materials. Composites Science and Technology, 68 (3-4) (2008) 953-962.

[9] V. Parameswaran and A. Shukla, Crack-Tip stress fields for dynamic fracture in functionally gradient materials. Mech. of Mater. 31 (1999) 579-596.

[10] K. H. Lee, Characteristics of a crack propagating along the gradient in functionally gradient materials. Int. J. Solids and Struct. 41 (2004) 2879-2898.

[11] L. B. Freund, Dynamic fracture mechanics, Cambridge University Press, Cambridge (1990).

[12] A. J. Rosakis, C. Liu and L. B. Freund, A note on the asymptotic stress field of a non-uniformly propagating dynamic crack. Int. J. of Fract. 50 (1991) R39-R45.

[13] A. Shukla and N. Jain, Dynamic damage growth in particle reinforced graded materials. Int. J. of Impact Engineering, 30 (2004) 777-803.

[14] V. B. Chalivendra and A. Shukla, Transient elastodynamic crack growth in functionally graded materials. J. Appl. Mech. 72 (2005) 237-248.

[15] K. H. Lee and G. S. Ban, Analysis of an unsteadily propagating crack under Mode I and II loading. J. of Mech. Sci. and Tech. 21 (2007) 403-414.

[16] K. H. Lee, J. S. Hawong and S. H. Choi, Dynamic stress intensity factors K_1, K_{11} and crack propagation characteristics of orthotropic materials. Engng. Fract. Mech., 53 (1996) 1,119-140.

[17] K. H. Lee, Stress and displacement fields for propagating the crack along the interface of dissimilar orthotropic materials under dynamic mode I and II load. ASME J. Appl. Mech. 67 (2000) 223-228.

Kwang-Ho Lee received a Ph.D. degree in Yeungnam University in 1993. Dr. Lee is currently a professor at the School of Mechanical and Automotive Engineering at Kyungpook National University in Korea. He also had worked in KOMSCO as an engineer and researcher (1982.3-1996.2). He is interested in the fields of fracture and stress analysis on the composite, interface, nano and functionally graded materials by theoretical and experimental mechanics. Specially, his major interest is analysis of dynamic crack tip fields.

Young-Jae Lee received his B.S degree in Agricultural Civil Engineering from Gyeongsang National University (GNU) in 1982. He then received his M.S. and Ph.D. degrees from GNU in 1984 and 1995, respectively. Dr. Lee is currently a professor at the department of Civil Engineering at Kyungpook National University in Korea. From 2005 to 2006, he had served as an editor of *Korea Institute for Structure Maintenance and Inspection.* His research interests are in the area of evaluation, diagnosis and optimum design of structure.

Sang-Bong Cho received a Ph. D. degree from Tokyo University in 1989. Dr. Cho is currently a professor at the division of Mechanical and Automation Engineering at Kyungnam University in Korea. His research interests are in the area of fracture mechanics, FEM stress analysis and fretting fatigue.